5-25-1961

Theory and Fabrication of Point Contact Diodes Utilizing Reduced Single Crystal Rutile TiO2

Goebel Davis Jr.

POINT CONTACT DIODES UTILIZING REDUCED SINGLE CRYSTAL RUTILE TiO_2 - DAVIS

THEORY AND FABRICATION OF POINT CONTACT DIODES UTILIZING REDUCED SINGLE CRYSTAL RUTILE TiO_2

By

Goebel Davis Jr.

A Thesis

Submitted in Partial Fulfillment of the

Requirements for the Degree of

Master of Science in Electrical Engineering

The University of New Mexico

1961

This thesis, directed and approved by the candidate's committee, has been accepted by the Graduate Committee of the University of New Mexico in partial fulfillment of the requirements for the degree of

MASTER OF SCIENCE

E F Castetter

Dean

May 25, 1961

Date

Thesis committee

W. W. Grannemann

Chairman

Ruben D. Kelly

E. S. Jordan

TABLE OF CONTENTS

ABSTRACT

Single crystal rutile TiO_2 upon reduction by heating in an atmosphere of hydrogen becomes a semiconductor, and the conductivity increases with the time and temperature of reduction. The reduction process creates oxygen vacancies with which there are associated two loosely bound electrons. These electrons may be raised to the conduction band by thermal excitation. Hence, an oxygen vacancy behaves like an impurity donor site.

Point contact diodes were made by utilizing reduced single crystal rutile; the laboratory fabrication techniques are described. For optimum rectification action, contact placement must be made on a mechanically undisturbed portion of a crystal formed by parting the crystal (after reduction) along a distinct, natural cleavage plane.

The volt-ampere averages of four typical diodes were used for curve fitting to the different theoretical models of diode operation. A selection of theoretical models for comparison with the observed phenomena requires that it be determined if minority carrier injection is occurring, and hence, if the system may or may not be regarded as a single-carrier system. A test for minority carrier injection was made by exploring the variation of potential in the neighborhood of a rectifying point contact. For an injecting contact, the local resistivity decreases for increasing forward current flow through the

Single crystal rutile TiO_2 upon reduction by heating in an atmosphere of hydrogen becomes a semiconductor, and the conductivity increases with the time and temperature of reduction. The reduction process creates oxygen vacancies with which there are associated two loosely bound electrons. These electrons may be raised to the conduction band by thermal excitation. Hence, an oxygen vacancy behaves like an impurity donor site.

Point contact diodes were made by utilizing reduced single crystal rutile; the laboratory fabrication techniques are described. For optimum rectification action, contact placement must be made on a mechanically undisturbed portion of a crystal formed by parting the crystal (after reduction) along a distinct, natural cleavage plane.

The volt-ampere averages of four typical diodes were used for curve fitting to the different theoretical models of diode operation. A selection of theoretical models for comparison with the observed phenomena requires that it be determined if minority carrier injection is occurring, and hence, if the system may or may not be regarded as a single-carrier system. A test for minority carrier injection was made by exploring the variation of potential in the neighborhood of a rectifying point contact. For an injecting contact, the local resistivity decreases for increasing forward current flow through the

rectifying contact. This phenomena was not observed, and hence, it is concluded that injection is not occurring to an extent which is experimentally detectable.

Diode Theory and Diffusion Theory equations for non-injecting contacts were fitted to the experimental data. In the forward direction, the Diode Theory equation fits the data exceptionally well, and the resultant equation is

$$I = 1.096 \times 10^{-8} \left[e^{12.39(V - 338.8I)} - 1 \right] \text{ (amperes), where}$$

V is the external applied voltage in volts.

In the reverse direction, the data was fitted to the Diode Theory equations and Diffusion Theory equations with Mott Barriers and Schottky Barriers. Corrections to these equations were made for the tunnel penetration or the image force. The resultant fits indicate (for both Diode and Diffusion Theory) that the rectification phenomena is most likely attributable to a Mott type barrier in which the image forces reduce the effective barrier height in the reverse direction.

CHAPTER I

INTRODUCTION

Point contact diodes have been made utilizing the n-type semiconductor, reduced single crystal rutile TiO_2. This report summarizes the results achieved, the techniques involved, and the theoretical tack taken to determine the most probable nature of the rectification phenomena occurring. The theoretical analysis is primarily limited to the aforementioned consideration; therefore, no detailed study of the variation of rectifier performance with frequency, temperature, etc., has been made.

The rectification process in crystals takes place in the immediate vicinity of the metal-semiconductor contact. In this region there exists a potential barrier (V_D) or "hump" of potential energy (eV_D). Rectification is believed to be a result of the asymmetrical distortion of this hump by the applied voltage.[1] In general, the higher the value of the equilibrium potential barrier, the better the rectifier.

For metal-semiconductor contacts, the two most often conjectured barrier forms are the Schottky type barrier and the Mott type barrier, For a Schottky barrier, the hump of potential energy is considered to be the result of differences between the thermionic work functions of the metal and semi-

---

[1]Torrey and Whitmer, Crystal Rectifiers, P. 68.

CHAPTER I

INTRODUCTION

Point contact diodes have been made utilizing the n-type semiconductor, reduced single crystal rutile TiO_2. This report summarizes the results achieved, the techniques involved, and the theoretical tack taken to determine the most probable nature of the rectification phenomena occurring. The theoretical analysis is primarily limited to the aforementioned consideration; therefore, no detailed study of the variation of rectifier performance with frequency, temperature, etc., has been made.

The rectification process in crystals takes place in the immediate vicinity of the metal-semiconductor contact. In this region there exists a potential barrier (V_D) or "hump" of potential energy (eV_D). Rectification is believed to be a result of the asymmetrical distortion of this hump by the applied voltage.[1] In general, the higher the value of the equilibrium potential barrier, the better the rectifier.

For metal-semiconductor contacts, the two most often conjectured barrier forms are the Schottky type barrier and the Mott type barrier. For a Schottky barrier, the hump of potential energy is considered to be the result of differences between the thermionic work functions of the metal and semi-

---

[1] Torrey and Whitmer, Crystal Rectifiers, P. 69.

conductor <u>or</u> to be caused by the presence of charged surface states at the semiconductor surface. For such type barriers, the barrier thickness increases with increasing reverse voltage and decreases with forward voltage. The existence of such a barrier of voltage dependent thickness was first suggested by Schottky. The Mott barrier is formed as a result of placing contacts on semiconductor surfaces which have non-uniform impurity distributions. The required non-uniformity is that the impurity density or conductivity should decrease with distance in going from the bulk of the semiconductor to the surface. The thickness of such a barrier is determined primarily by the thickness of the pure region and is only slightly altered for reverse applied voltages.

In practice, the barrier potential does not maintain its high value for reverse voltage which the idealized theoretical equations predict. For reverse voltages, decreasing values of V_D imply increasing reverse leakage currents. In practical cases, the idealized reverse direction equations must be corrected by adjustment of the value of eV_D. The resulting effective lowering of the barrier height is usually attributed to one of two effects: the electron image force or the electron tunnel penetration of the barrier.

An electron at a distance x from the metal contact (within the semiconductor) induces a positive charge on the metal surface and it is thus attracted to it. This positive charge

is referred to as the image, and the attractive force is called the image force. This force, which results in an effective lowering of the barrier height for reverse applied voltages, is usually neglected in the development of the idealized equations.[2]

In accordance with classical principles, an electron can pass a potential barrier of height V only if its kinetic energy exceeds a definite minimum given by

$$1/2mv^2 \geq eV.$$

However, a wave-mechanical analysis of the problem shows that an electron which has insufficient energy to pass over the barrier has a definite non-zero chance of passing through it. This is known as the tunnel effect. With the appropriate circumstances, the tunnel effect lowers the barrier height of a diode for reverse directions. In the correction factors for this phenomena, it is usually assumed that the barrier is completely opaque if its thickness for electrons of a given energy is greater than a certain critical value x_c and completely transparent if the thickness is smaller than x_c.[3]

One of the first considerations in the selection of theoretical models of diode operation is the determination of

---

[2]Henisch, H. K., Rectifying Semi-Conductor Contacts.

[3]Ibid.

is referred to as the image, and the attractive force is called the image force. This force, which results in an effective lowering of the barrier height for reverse applied voltages, is usually neglected in the development of the idealized equations.[2]

In accordance with classical principles, an electron can pass a potential barrier of height V only if its kinetic energy exceeds a definite minimum given by

$$1/2mv^2 \geq eV.$$

However, a wave-mechanical analysis of the problem shows that an electron which has insufficient energy to pass over the barrier has a definite non-zero chance of passing through it. This is known as the tunnel effect. With the appropriate circumstances, the tunnel effect lowers the barrier height of a diode for reverse directions. In the correction factors for this phenomena, it is usually assumed that the barrier is completely opaque if its thickness for electrons of a given energy is greater than a certain critical value x_c and completely transparent if the thickness is smaller than x_c.[3]

One of the first considerations in the selection of theoretical models of diode operation is the determination of

---

[2] Henisch, H. K., <u>Rectifying Semi-Conductor Contacts</u>.

[3] Ibid.

whether minority carrier injection is occurring, and hence, if the system may or may not be regarded as a single-carrier system. This question is resolved in Chapter III before the theoretical model development in Chapter IV.

As is characteristic of the whole field of solid-state engineering, minor changes in the processes involved in making these diodes can radically change the results. Hence, in the next chapter, an attempt is made to document the procedures involved.

CHAPTER II

CRYSTAL THEORY, PREPARATION AND MOUNTING

All of the experimental work has been done on synthetic single crystals of rutile TiO_2 supplied by Linde Air Products Company. These crystals, while relatively pure, are far from the purities presently achievable in germanium and silicon single crystals. Spectroscopic analyses of Linde crystals (by the National Bureau of Standards) showed a Ba impurity of 0.01 percent, minor impurities of Al and Mg present in amounts of 0.001 to 0.01 percent, and traces of Ag, Cu, Ca, Fe, and Pb. The alkalies, if present, were in amounts less than 0.05 percent.[1] The results obtained with these crystals might be considerably modified if crystals of higher purity were available.

Linde single crystal rutile TiO_2 has a resistivity of about 10^{13} ohm-cm at room temperature.[2] Pure rutile TiO_2 can be converted into a semiconductor in numerous ways; however, all methods fall into two general categories:[3]

a. Creation of oxygen vacancies, and

b. Contamination of the TiO_2 with foreign molecules.

The second procedure has not been attempted, but the first method has been successfully utilized numerous times. Samples

---

[1]Breckenridge and Hosler, Phys. Rev. 41, 793 (1953).

[2]From measurements made by W.H. Closser at Sandia Corp.

[3]F. A. Grant, Properties of Rutile TiO_2, N.B.S, Jan. 15, 1959.

CHAPTER II

CRYSTAL THEORY, PREPARATION AND MOUNTING

All of the experimental work has been done on synthetic single crystals of rutile TiO_2 supplied by Linde Air Products Company. These crystals, while relatively pure, are far from the purities presently achievable in germanium and silicon single crystals. Spectroscopic analyses of Linde crystals (by the National Bureau of Standards) showed a Ba impurity of 0.01 percent, minor impurities of Al and Mg present in amounts of 0.001 to 0.01 percent, and traces of Ag, Cu, Ca, Fe, and Pb. The alkalies, if present, were in amounts less than 0.05 percent.[1] The results obtained with these crystals might be considerably modified if crystals of higher purity were available.

Linde single crystal rutile TiO_2 has a resistivity of about 10^{13} ohm-cm at room temperature.[2] Pure rutile TiO_2 can be converted into a semiconductor in numerous ways; however, all methods fall into two general categories:[3]

a. Creation of oxygen vacancies, and

b. Contamination of the TiO_2 with foreign molecules.

The second procedure has not been attempted, but the first method has been successfully utilized numerous times. Samples

---

[1] Breckenridge and Hosler, Phys. Rev. 41, 793 (1953).

[2] From measurements made by W.H. Closser at Sandia Corp.

[3] F. A. Grant, Properties of Rutile TiO_2, N.B.S. Jan. 15, 1959.

have been produced with resistivities as low as 0.02 ohm-cm or more, depending on (and decreasing with) the time and temperature of reduction. This reduction is a treatment which will cause a loss of oxygen (or excess of titanium), and is achieved by heating the rutile sample in a low oxygen pressure or in an atmosphere of hydrogen. The reduced rutile becomes an n-type semiconductor with physical properties which depend on the oxygen loss.[4]

"Associated with every oxygen vacancy there are two loosely bound electrons, which may be raised to the conduction band by thermal excitation at higher temperatures. In effect, therefore, an oxygen vacancy behaves like an impurity site; the corresponding ionization potentials are believed to be less than one electron volt, and may even be very much smaller.[5] Additionally, the results of the experiment on injection of minority carriers indicate that the role of the minority carriers (in this case holes) may be neglected in the conduction process.

The same crystals were used for both the injection test and the diode fabrication and were prepared as follows:

1) Circular discs of rutile (about 0.1 inch thick) were cut by a diamond tipped saw blade from a single crystal

---

[4] Breckenridge, op.cit.

[5] Grant, op.cit.

of rutile. The slices were made along planes perpendicular to the central or major axis.

2) These high resistivity samples were then reduced to a semiconductor by heating in a hydrogen atmosphere. The hydrogen used was commercial quality dry hydrogen supplied by Linde. The samples were then placed in a Coors Volcanus combustion tube for confinement of the hydrogen, and the whole assembly was heated in a Haskins electric furnace. The temperature was manually controlled by a Variac with the aid of a chromel-alumel thermocouple placed in proximity to the sample within the combustion tube. In order to control the level of reduction more precisely, Linde commercial quality dry nitrogen was passed through the combustion tube during the warm-up and cool-down periods. Hence, a reduction at 800°C for ten minutes was achieved by cutting off the nitrogen when the temperature had stabilized at 800°C and switching on the hydrogen. At the end of ten minutes, the nitrogen was switched on again and left on until the samples had cooled.

3) Ohmic-low resistance base contacts were achieved by attaching two copper wires to opposite edges of the samples with thermo setting conductive epoxy glue made from one part Hysol 3475 Hardener, four parts Hysol 2038, and five parts (by weight) of finely ground silver powder. However, without additional processing, the contacts have rather high resistances. Apparently,

high resistance surface films are present which have to be broken down in some manner. The formation of these surface films might be associated with the imperfect reduction process involving the commercial quality gasses.
The contacts were made low resistant and ohmic by passing about 0.2 amperes of current through them until a pronounced breakdown and reduction of resistance was noted.

4) It has been observed experimentally that good point contact diodes rarely are achieved when a contact is placed on a rutile surface which was directly exposed to the reduction environment. This might be a consequence of the high resistance surface film described in 3). However, consistently good diodes are achieved when the crystal contacting region is a clean cleaved surface (cleaved after the reduction is accomplished). There are several distinct natural cleavage planes in single crystal rutile, and in general, the crystals may be readily parted. For the samples in question, the semiconductor discs were merely given a sharp blow with a knife edge and a smooth cleaved surface resulted.

5) The half disc-shaped samples, with an ohmic lead attached, were then glued to rectangular aluminum base mounts suitable for attaching to the microscope and micro-manipulator assembly described in Chapter III. The crystal mounting was made at an angle such that the cleaved surface was suitably positioned for contact placement.

If the initially clean cleaved crystal surface is contaminated by touching with the fingers or otherwise, its rectifying ability can be restored by washing in HCl followed by about a twelve-hour rinse in distilled water. After pulling the moisture out of the crystal by placing it in a vacuum, the sample may be re-used with no apparent degradation of its characteristics.

CHAPTER III

TEST FOR CONTACT INJECTION

This chapter describes the experimental tests performed to ascertain if the rectifying contacts analyzed were injecting minority carriers into the bulk material. An assessment of this type is limited by the sensitivity of the experimental technique, since the surface purity or surface minority carrier recombination center density and minority carrier mobility affect the detection of the injection process. These contacts which are now classified as non-injecting as a result of this experiment may, in fact, be injecting to an extent beyond the limits of experimental detection. When "single crystal" rutile TiO_2 of high purity becomes available, injection might occur and be experimentally detectable.

The experimental technique used was one originally employed by Brattain and Bardeen.[1] The presence of injected minority charge carriers is detected by measuring the decrease in the semiconductor resistivity in the immediate vicinity of a rectifying point contact which is injecting. This is accomplished by determining the variation of potential (V) in the neighborhood of a rectifying point contact carrying a forward current (I) by measuring the open circuit voltage (V) between a second non-

---

[1]Brattain, W. H. and Bardeen, J. Phys. Rev. 74,231 (1948)

rectifying potential probe and the common base. For a material of constant resistivity, the ratio $\frac{2\pi rV}{I}$ should be independent of I and r and should be equal in magnitude to the bulk resistivity. The derivation of this expression follows from the definition of resistivity and the assumption of a constant resistivity and a hemispherically constant radial current flow. Resistivity is the ratio of voltage gradient to current density. The voltage gradient is, hence, under the stated assumptions equal to $\frac{V}{r}$. The current density, j, is given by the total current divided by the area of a hemisphere of radius r. Thus,

$$j = \frac{I}{2\pi r^2}.$$

The resulting expression for resistivity is

$$\rho = \frac{V/r}{I/2\pi r^2} = \frac{2\pi rV}{I}.$$

For an injecting contact, the ratio $\frac{2\pi rV}{I}$ is found to decrease for increasing values of I. This change is due to an increase in the concentration of carriers in the vicinity of the rectifying point contact for increasing forward bias.

In Brattain and Bardeen's original experiment, the value of $\frac{2\pi rV}{I}$ also decreased with decreasing separation distances (r) between the rectifying and nonrectifying contacts. This variation was attributed to different impurity concentrations in the bulk material and the semiconductor surface. As will be presently shown, this same form of variation of $\frac{2\pi rV}{I}$ with r was present in the injection test on TiO_2. This decrease in resistivity with decreasing values of r is most likely due to the presence of a surface layer or film which has a higher value of resistivity than the bulk resistivity of the semiconductor. This explanation is plausible, considering the

rectifying potential probe and the common base. For a material of constant resistivity, the ratio $\frac{2\pi r V}{I}$ should be independent of I and r and should be equal in magnitude to the bulk resistivity. The derivation of this expression follows from the definition of resistivity and the assumption of a constant resistivity and a hemispherically constant radial current flow. Resistivity is the ratio of voltage gradient to current density. The voltage gradient is, hence, under the stated assumptions equal to $\frac{V}{r}$. The current density, j, is given by the total current divided by the area of a hemisphere of radius r. Thus,

$$j = \frac{I}{2\pi r^2}.$$

The resulting expression for resistivity is

$$\rho = \frac{V/r}{I/2\pi r^2} = \frac{2\pi r V}{I}.$$

For an injecting contact, the ratio $\frac{2\pi r V}{I}$ is found to decrease for increasing values of I. This change is due to an increase in the concentration of carriers in the vicinity of the rectifying point contact for increasing forward bias.

In Brattain and Bardeen's original experiment, the value of $\frac{2\pi r V}{I}$ also decreased with decreasing separation distances (r) between the rectifying and nonrectifying contacts. This variation was attributed to different impurity concentrations in the bulk material and the semiconductor surface. As will be presently shown, this same form of variation of $\frac{2\pi r V}{I}$ with r was present in the injection test on TiO_2. This decrease in resistivity with decreasing values of r is most likely due to the presence of a surface layer or film which has a higher value of resistivity than the bulk resistivity of the semiconductor. This explanation is plausible, considering the

Table I Test A for Injection Experimental Data

r(cm)	I (amps)	V (volts)	$\rho = \frac{2\pi r V}{I}$	I	V	$\rho = \frac{2\pi r V}{I}$	I	V	$\rho = \frac{2\pi r V}{I}$
0.039	0.0002	0.01	12.25	0.001	0.08	14.7	0.002	0.13	15.90
0.034	"	0.01	10.7	"	0.07	14.95	"	0.14	14.95
0.029	"	0.01	9.1	"	0.07	12.8	"	0.14	12.75
0.024	"	0.01	7.5	"	0.07	10.55	"	0.14	10.55
0.019	"	0.01	6.0	"	0.08	9.55	"	0.15	9.0
0.014	"	0.01	4.4	"	0.085	7.5	"	0.165	7.25
0.009	"	0.02	5.65	"	0.09	5.1	"	0.18	5.1

Table II Test B for Injection Experimental Data

Test No.	r (cm)	I (amps)	V (volts)	$\rho = \frac{2\pi rV}{I}$	I	V	$\rho = \frac{2\pi rV}{I}$	I	V	$\rho = \frac{2\pi rV}{I}$
1	0.006	0.0005	0.04	3.01	0.001	0.09	3.39	0.0016	0.135	3.18
		0.0022	0.185	3.17	0.0026	0.22	3.19	0.003	0.25	3.12
		0.0035	0.28	3.01	0.004	0.32	3.01	0.005	0.415	3.13
2	0.0065	0.0005	0.04	3.27	0.001	0.085	3.47	0.0016	0.12	3.06
		0.0022	0.17	3.16	0.0026	0.20	3.14	0.003	0.23	3.13
		0.0035	0.27	3.15	0.004	0.31	3.16	0.005	0.40	3.27
3	0.007	0.0005	0.03	2.64	0.001	0.07	3.08	0.0016	0.10	2.75
		0.0022	0.14	2.80	0.0026	0.17	2.88	0.003	0.19	2.78
		0.0035	0.23	2.89	0.004	0.265	2.92	0.005	0.335	2.95
4	0.0065	0.0005	0.035	2.86	0.001	0.075	3.06	0.0016	0.115	2.93
		0.0022	0.16	2.97	0.0026	0.19	2.98	0.003	0.22	2.99
		0.0035	0.26	3.03	0.004	0.30	3.06	0.005	0.38	3.11
5	1.007	0.0005	0.03	2.64	0.001	0.07	3.08	0.0016	0.105	2.89
		0.0022	0.145	2.90	0.0026	0.175	2.96	0.003	0.20	2.93
		0.0035	0.24	3.02	0.004	0.28	3.08	0.005	0.355	3.12
6	0.006	0.0005	0.05	3.77	0.001	0.10	3.77	0.002	0.20	3.77
		0.003	0.30	3.77	0.004	0.405	3.82			
7	0.006	0.0005	0.045	3.39	1.001	0.095	3.58	0.002	0.195	3.68
		0.003	0.29	3.64	0.004	0.38	3.58			
8	0.006	0.0005	0.04	3.02	0.001	0.09	3.39	0.002	0.185	3.48
		0.003	0.28	3.52	0.004	0.37	3.48			
9	0.006	0.0005	0.05	3.77	0.001	0.09	3.39	0.002	0.18	3.39
		0.003	0.26	3.27	0.004	1.355	3.34			

charge transport mechanism involving oxygen vacancy centers with associated free donor electrons. Hence, oxygen vacancy centers near the surface of the material may be slowly refilled by room temperature oxidation which would result in a higher surface resistivity.

Fortunately, however, variations of $\frac{2\pi rV}{I}$ with r are not directly relevant to the test for injection. The important criterion for injection to be present is the occurrence of a statistically significant decrease of $\frac{2\pi rV}{I}$ with increasing values of I (with r being held constant). As will be shown, this type of variation was not present.

The tests for injection of minority carriers were made on the same semiconductor surfaces that were used to make the diodes whose V-I characteristics were used in the analysis and curve fitting process. The mounted crystals were rigidly attached to the observation platform of an 80 power microscope in a position such that the crystal surface could be brought into focus and observed. Mechanical stages or micromanipulators were used for the positioning of the point contacts on the crystal surface. Independent three-dimensional positioning was achievable for each point contact.

Copper wire and tungsten wire were used, respectively, for the rectifying and non-rectifying contacts. Both contacts were relatively blunt with a necked down wire diameter of approximately 0.008 cm at the tips or contact points. To rid the contacts of any foreign contamination, they were cleaned in an HCl solution before mounting and then rinsed in distilled water. This processing is, in general, essential to the achieving of a good diode.

The V-I characteristics of the contacts, with a 500 cps AC voltage applied, were displayed on an oscilloscope during the positioning of the contacts. For a rectifying contact, the pressure and lateral positioning were adjusted until a favorable rectifying characteristic was observed. For the non-rectifying contact, the required point position was usually predetermined by the position of the rectifying contact. In general, the characteristic of the tungsten wire when first placed on the semiconductor surface was non-rectifying, symmetrical about the zero axis, but non-linear, i.e., the characteristic was not a straight line function. The required linear, ohmic contact characteristic (a straight line oscilloscope display), was achieved by capacitor discharge forming. Usually, one or two discharges of a 0.01 μf capacitor charged to between 50 to 100 volts would change the characteristic from non-linear to linear.

Figure I shows an electrical schematic of the test circuit used. The complexity of the test necessitated the use of a switching circuit for the various required functions. The general procedure followed was:

1) The switch was put in position 4 (see Figure I) and the rectifying point contact was adjusted to achieve good rectification action.
2) The ohmic probe was adjusted to the desired position above the surface by visual observation through the microscope and by the indication of the index head graduation on the micromanipulator.
3) The ohmic probe was lowered to the surface of the crystal. If the ohmic and rectifying probe were in very close proximity, switching to position 1 would

The V-I characteristics of the contacts, with a 500 cps AC voltage applied, were displayed on an oscilloscope during the positioning of the contacts. For a rectifying contact, the pressure and lateral positioning were adjusted until a favorable rectifying characteristic was observed. For the non-rectifying contact, the required point position was usually predetermined by the position of the rectifying contact. In general, the characteristic of the tungsten wire when first placed on the semiconductor surface was non-rectifying, symmetrical about the zero axis, but non-linear, i.e., the characteristic was not a straight line function. The required linear, ohmic contact characteristic (a straight line oscilloscope display), was achieved by capacitor discharge forming. Usually, one or two discharges of a 0.01 μf capacitor charged to between 50 to 100 volts would change the characteristic from non-linear to linear.

Figure I shows an electrical schematic of the test circuit used. The complexity of the test necessitated the use of a switching circuit for the various required functions. The general procedure followed was:

1) The switch was put in position 4 (see Figure I) and the rectifying point contact was adjusted to achieve good rectification action.

2) The ohmic probe was adjusted to the desired position above the surface by visual observation through the microscope and by the indication of the index head graduation on the micromanipulator.

3) The ohmic probe was lowered to the surface of the crystal. If the ohmic and rectifying probe were in very close proximity, switching to position 1 would

Figure I - Contact Injection Test Circuit and Description

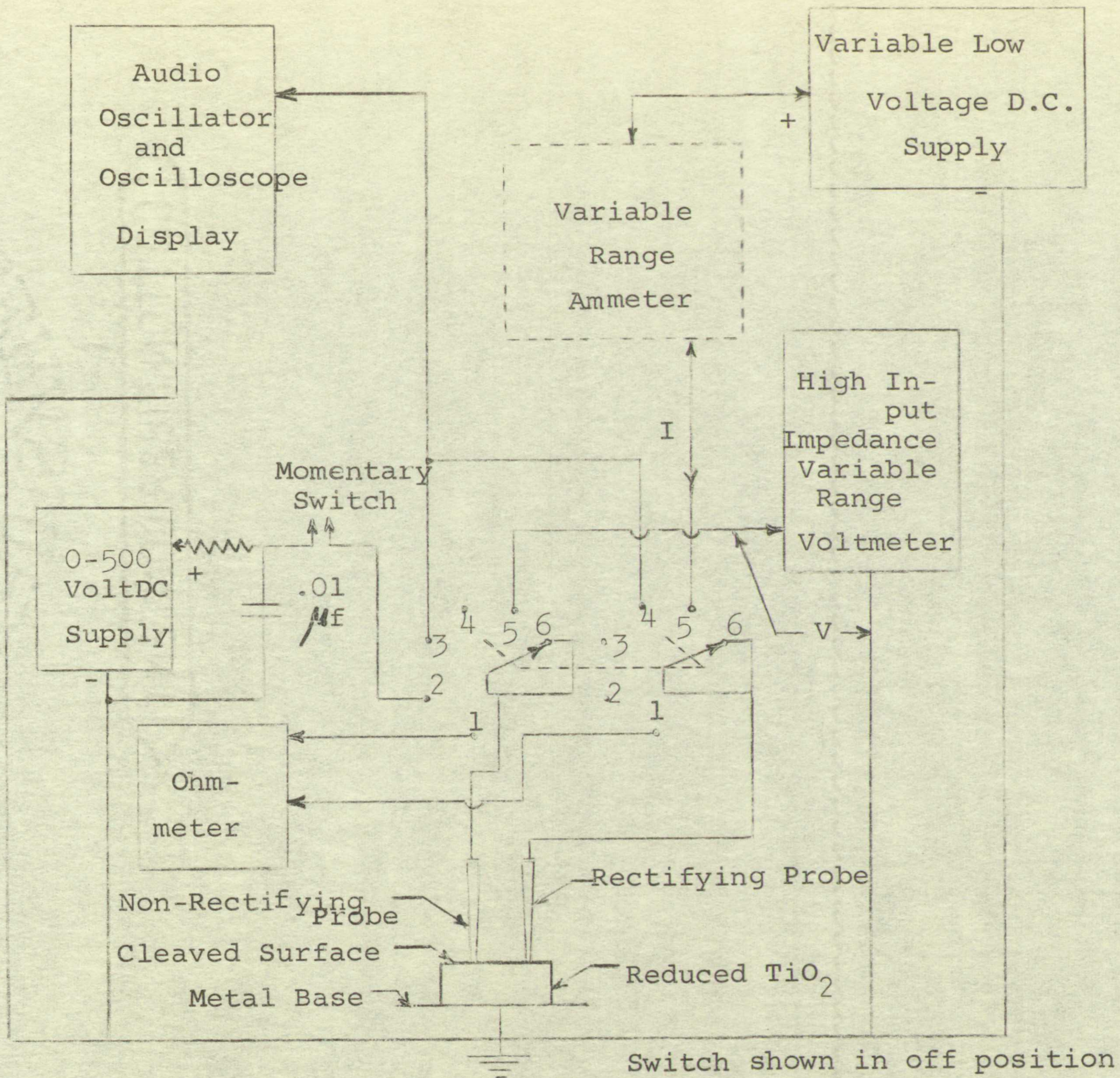

SWITCHING CIRCUITS

Switch Position	FUNCTION
1	Ohmmeter short test between probes
2	Capacitor discharge forming of non-rectifying potential probe contact
3	Oscilloscope display of the non-rectifying contact V-I characteristic
4	Oscilloscope display of the rectifying contact V-I characteristic
5	Voltage applied to the rectifying contact and simultaneous $V_{(r)}$ and I readings may be taken
6	OFF or no connections made to the contact probes

detect a short occurring between the two probes, if it occurred. If shorting occurred, the ohmic probe was moved slightly. When the ohmic probe had been properly positioned without shorting occurring, the switch was put in position 3 where a check was made of the linearity of the ohmic contact. If it was not linear, the switch was placed in position 2 where a momentary contact switch could be pushed to apply a forming voltage pulse. The success of the forming action could be immediately determined by observing the contact V-I display (i.e., Position 3).

4) When the contact had been formed to a low enough linear resistance, the voltage and current readings were taken by switching to position 5. The different required levels of current through the rectifying contact were developed by varying the applied low voltage DC to the rectifier.

5) If readings at different distances from the rectifying contacts were desired, the ohmic contact was repositioned to the desired spot and the procedure outlined above starting at Step 3 was repeated.

In Tables I and II are tabulated the experimental data taken and the associated calculations of $\rho = \frac{2\pi rV}{I}$. Two sets of data were taken, Test A with variable I and r, and Test B with variable I and constant r. The data for the A test was taken primarily to see if the value of $\frac{2\pi rV}{I}$ decreased with decreasing probe separation distances r, in the same manner as was experienced by Brattain and Bardeen. The A-Test data is tabulated in Table I. Note the consistent decrease of ρ with decreasing r except for the test at the 0.0002 ampere and

detect a short occurring between the two probes, if it occurred. If shorting occurred, the ohmic probe was moved slightly. When the ohmic probe had been properly positioned without shorting occurring, the switch was put in position 3 where a check was made of the linearity of the ohmic contact. If it was not linear, the switch was placed in position 2 where a momentary contact switch could be pushed to apply a forming voltage pulse. The success of the forming action could be immediately determined by observing the contact V-I display (i.e., Position 3).

4) When the contact had been formed to a low enough linear resistance, the voltage and current readings were taken by switching to position 5. The different required levels of current through the rectifying contact were developed by varying the applied low voltage DC to the rectifier.

5) If readings at different distances from the rectifying contacts were desired, the ohmic contact was repositioned to the desired spot and the procedure outlined above starting at Step 3 was repeated.

In Tables I and II are tabulated the experimental data taken and the associated calculations of $\rho = \frac{2\pi r V}{I}$. Two sets of data were taken, Test A with variable I and r, and Test B with variable I and constant r. The data for the A test was taken primarily to see if the value of $\frac{2\pi r V}{I}$ decreased with decreasing probe separation distances r, in the same manner as was experienced by Brattain and Bardeen. The A-Test data is tabulated in Table I. Note the consistent decrease of ρ with decreasing r except for the test at the 0.0002 ampere and

$r = 0.009$ cm level. At this low level, the values of V could not be accurately determined because of the equipment limitations, which should account for this one observed inconsistency. Note also that above the 0.0002 ampere level, the calculated values of ρ are (within equipment error limitations) constant for constant r and increasing values of I. Hence, the A-Test data is consistent in regard to the hypothesis that injection is not occurring.

The data for the more complete and conclusive test for injection is presented in Table II. If injection were occurring, the effects would be most pronounced at small values of separation distances, r. For this reason, the nine independent checks of Test B were made with the minimum separation distances which could be achieved without the ohmic probe shorting to the rectifying probe. The procedure followed was to first position the ohmic and rectifying probes in such close proximity that shorting occurred. The ohmic probe was then shifted away from the rectifying probe the minimum distance required for shorting to cease. This required shift (as indicated by the micro-manipulator) was between 0.001 and 0.002 cm. Note that none of the indicated values of r in the tables are this small. The reason for this is that the precise value of r cannot be determined because of the finite diameter of the probes. Hence, as a first approximation, 0.005 cm (i.e., about one-half of a point diameter) has been added to the position distances indicated by the micro-manipulator. Fortunately, errors in the values of r cannot affect the conclusion because r is held constant while I is varied. The important result to be noted is that for each of

r = 0.009 cm level. At this low level, the values of V could not be accurately determined because of the equipment limitations, which should account for this one observed inconsistency. Note also that above the 0.0002 ampere level, the calculated values of ρ are (within equipment error limitations) constant for constant r and increasing values of I. Hence, the A-Test data is consistent in regard to the hypothesis that injection is not occurring.

The data for the more complete and conclusive test for injection is presented in Table II. If injection were occurring, the effects would be most pronounced at small values of separation distances, r. For this reason, the nine independent checks of Test B were made with the minimum separation distances which could be achieved without the ohmic probe shorting to the rectifying probe. The procedure followed was to first position the ohmic and rectifying probes in such close proximity that shorting occurred. The ohmic probe was then shifted away from the rectifying probe the minimum distance required for shorting to cease. This required shift (as indicated by the micro-manipulator) was between 0.001 and 0.002 cm. Note that none of the indicated values of r in the tables are this small. The reason for this is that the precise value of r cannot be determined because of the finite diameter of the probes. Hence, as a first approximation, 0.005 cm (i.e., about one-half of a point diameter) has been added to the position distances indicated by the micro-manipulator. Fortunately, errors in the values of r cannot affect the conclusion because r is held constant while I is varied. The important result to be noted is that for each of

the nine checks made, V/I is relatively constant for fixed r.

Analysis of the calculated values of ρ indicates that no statistically significant deviation of ρ is present. Hence, it is concluded that injection is not taking place to an extent which is experimentally detectable.

CHAPTER IV

DIODE THEORY AND DIFFUSION THEORY*

As a result of the contact injection experiment (see Chapter III) which yielded no indication of the presence of injected minority carriers (holes in this case), the theoretical models developed can be restricted to those associated with single carrier systems. The equations are developed for the electron single carrier system, but with only minor modifications, these equations would apply to hole single carrier systems.

Metal to semiconductor diode rectification involves the activation of charge carriers over the rectification barrier. Two different assumptions can be made as to the manner in which this is done, and two different theories result. One, the Diode Theory, involves the assumption that collisions within the barrier may be neglected. The other, the Diffusion Theory, is based on the assumption that the barrier thickness is large compared with the electron mean free path and hence that the electrons experience numerous collisions within the barrier.

A - Diode Theory

From Henisch, the probability of finding an electron which has velocity components between v_x and $(v_x + dv_x)$, v_y and $(v_y + dv_y)$, v_z and $(v_z + dv_z)$ is given by

$$dn = \left(\frac{m^*}{2\pi KT}\right)^{3/2} \exp\left[\frac{-m\ v_x^{\ 2} + v_y^{\ 2} + v_z^{\ 2}}{2\ KT}\right] dv_x\ dv_y\ dv_z, \text{ where}$$

*The derivations of this appendix are modified and abbreviated forms of those appearing in Chapter 7 of Rectifying Semi-Contacts by H. K. Henisch.

n = total concentration of electrons

m^* = electron effective mass

K = Boltzmann's constant

T = absolute temperature

v_i = electron velocity components

It has been shown[1] that the velocity distributions are independent in the different directions and, hence, that the right side of equation(1) can be regarded as the product of three probabilities. For a planor diode with positive x distances defined as being along the perpendicular going into the semiconductor, the only velocity of interest is v_x. Hence,

$$\left.\begin{array}{l}\text{the incremental concentration}\\ \text{of electrons moving in}\\ \text{the x direction}\end{array}\right) = n\left(\frac{m^*}{2\pi KT}\right)^{1/2} \exp\left(\frac{-m^* v_x^2}{2\ KT}\right) dv_x$$

and

$$\left.\begin{array}{l}\text{the incremental number of}\\ \text{electrons which cross unit}\\ \text{area of cross-section in}\\ \text{unit time}\end{array}\right) = nv_x\left(\frac{m^*}{2\pi KT}\right)^{1/2} \exp\left(\frac{-m^* v_x^2}{2\ KT}\right) dv_x.$$

In the bulk of the semiconductor, for no voltages applied (because of equilibrium considerations) there are zero net electrons crossing any given cross-sectional area. However, for a barrier of thickness λ with a voltage applied, there is a non-zero net passage of electrons. Under the assumption that collisions within the barrier may be neglected, any electron which crosses the plane $x = \lambda$ with a sufficient

---

[1] J. Jeans, An Introduction to the Kinetic Theory of Gases, Cambridge Univ. Press, 1940.

velocity in the negative x direction will reach the metal. This required minimum velocity is given by,

$$1/2\ m^*v_{xo}^2 = e(v_D + V),$$

where V_D is the diffusion voltage developed by the rectification barrier, and V is the potential difference across the barrier layer of a rectifier resulting from the application of an external voltage (V does not include the IR drop).

As each electron carries a charge e, the current density j_1 due to electrons which have velocities above the required minimum is,

$$j_1 = ne \left(\frac{m^*}{2\pi KT}\right)^{1/2} \int_{-v_{xo}}^{-\infty} v_x \exp\left(-m^*v_x^{\ 2}/2KT\right) dv_x,$$

or

$$j_1 = ne \left(\frac{KT}{2\pi m^*}\right)^{1/2} \exp\left(\frac{-m^*v_{xo}^{\ 2}}{2KT}\right)$$. Using the relation

$$1/2\ m^*v_{xo}^{\ 2} = e(V_D + V),$$

$$j_1 = ne\left(\frac{KT}{2\pi m^*}\right)^{1/2} \exp\left[\frac{-e\left(V_D + V\right)}{2KT}\right].$$

The net flow of electrons across the barrier in the opposite direction when V = 0 or equilibrium prevails is given by,

$$j_2 = -ne\left(\frac{KT}{2\pi m^*}\right)^{1/2} \exp\left(\frac{-eV_D}{KT}\right)$$. The total current

density j_d is given by the sum of j_1 and j_2. Thus

$$-j_d = ne\left(\frac{KT}{2\pi m^*}\right)^{1/2} \exp\left(\frac{-eV_D}{KT}\right) \left[1 - \exp\left(\frac{-eV}{KT}\right)\right],$$

or converting to total current j, by multiplying j_d by the barrier area, a,

$$j = ane\left(\frac{KT}{2\pi m^*}\right)^{1/2} \exp\left(\frac{-eV_D}{KT}\right) \left[\exp\left(\frac{-eV}{KT}\right) - 1\right] \tag{1}$$

Equation(1) is the general uncorrected Diode Theory equation. Note that positive values of V correspond to the reverse direction of current flow and negative values to the forward direction. Note also that for large reverse direction applied voltages, the current magnitude approaches a saturation value A, where

$$A = ane\left(\frac{KT}{2\pi m^*}\right)^{1/2} \exp\left(\frac{-eV_D}{KT}\right).$$ Thus equation (1) may be rewritten as,

$$j = A\left[\exp\left(\frac{-eV}{KT}\right) - 1\right]. \tag{2}$$

In practical cases the forward direction current is better described by

$$I = A\left\{\exp\left[\alpha(V-IR)\right] - 1\right\}, \text{ where} \tag{3}$$

I = positive forward current flowing

V = total external positive applied voltage

R = total diode linear or spreading resistance

α = a fitted parameter.

Equation (3) is used in the forward direction curve fitting in Chapter V. Equation (2), with appropriate modifications, is the form used for the Diode Theory reverse direction analysis and curve fitting.

In practice, Equation (2) will not describe the observed phenomena without modification, as the observed current does not saturate to A but rather continues to increase for increasing reverse voltages. Corrections for the image force and tunnel penetration improve the accuracy of the fit. The image force and tunnel penetration result in a lowering of the effective barrier height, V_D, with increasing reverse voltage. Hence as an approximate correction, the term eV_D in Equation (2) can be replaced by $eV_D - \Delta\emptyset$, where $\Delta\emptyset$ is the diminuation of barrier height.

For a Schottky barrier, $\Delta\emptyset$ is found from Equations 734.5 and 743.1 of Henisch for the image force and tunnel effect corrections respectively.

They are:

$$\Delta\emptyset = \left[\left(V_D + V\right)e^{7}\pi \frac{N}{2k^3}\right]^{1/4} \quad \text{for the image force, and}$$

$$\Delta\emptyset = \left[\frac{8\pi Ne^3\left(V_D + V\right)}{k}\right]^{1/2} \cdot \; x_c \quad \text{for the tunnel effect,}$$

where N is the total concentration of electrons, and x_c is the critical thickness below which a barrier can be considered as being completely transparent to electrons.

These corrections are now applied to Equation (2) and for convenience the sign of j is kept positive. The term $\left[\exp\left(\frac{-eV}{KT}\right) - 1\right]$ is not included as its value is effectively

-1 for reverse voltages greater than about 0.5 volts.

Hence, in the reverse direction for an image force corrected Schottky barrier, the Diode Theory predicts:

$$j = A \exp \left\{ \left[\left(V_D + V \right) e^7 \pi \frac{N}{2k^3} \right]^{1/4} \cdot \frac{1}{KT} \right\}. \qquad (4)$$

And, in the reverse direction for a tunnel effect corrected Schottky barrier, the Diode Theory predicts:

$$j = A \exp \left\{ \left[\left(V_D + V \right) 8 e^3 \pi \frac{N}{k} \right]^{1/2} \cdot \frac{x_c}{kT} \right\}. \qquad (5)$$

For a Mott barrier, the corrections are essentially the same as above. For this type barrier, the electric field in the barrier is simply $F = - \left(\frac{V_D + V}{\lambda_o} \right)$, the barrier thickness λ_o being a constant for reverse voltages. From Henisch (equation 722.6),

$\Delta\phi = (-F)^{1/2} k^{-1/2} e^{3/2}$ for the image force correction,

and thus,

$$\Delta\phi = \left[\frac{\left(V_D + V \right) e^3}{k\lambda_o} \right]^{1/2} .$$

From Henisch (equation 743.3),

$\Delta\phi = e \left(V_D + V \right) \frac{x_c}{\lambda_o}$ for the tunnel effect correction.

These corrections are now applied to Equation(2) in like manner as for the Schottky barrier.

Hence, in the reverse direction for an image force corrected Mott barrier, the Diode Theory predicts:

$$j = A \exp \left\{ \left[e^3 \left(V_D + V\right) \frac{1}{k\,\lambda_o} \right]^{1/2} \cdot \frac{1}{KT} \right\}. \tag{6}$$

And, in the reverse direction for a tunnel effect corrected Mott barrier, the Diode Theory predicts:

$$j = A \exp \left\{ \left[e \left(V_D + V \right) \frac{x_c}{\lambda_o} \right] \cdot \frac{1}{KT} \right\}. \tag{7}$$

Equations (4), (5), (6), and (7) are the Diode Theory relations used in the reverse direction curve fitting in Chapter VI.

B - Diffusion Theory.

The simple Diffusion Theory equations suitable for prediction of the forward direction characteristics did not fit the experimental data satisfactorily, while the Diode Theory equations yielded an exceptionally good fit (see Chapter V). Hence, the simple Diffusion Theory equations will be presented without proof and then modified for the reverse direction in the same manner as the Diode Theory.

The following Diffusion Theory equations are, respectively, Equations 763.1 and 763.2 from Henisch modified for total currents rather than current densities:

The simple diffusion characteristic of a Mott Barrier is:

$$j = a\sigma \frac{V_D + V}{\lambda_o} \exp \left(\frac{-eV_D}{KT} \right) \left[1 - \exp \left(\frac{-eV}{KT} \right) \right] , \tag{8}$$

and the simple diffusion characteristic of a Schottky Barrier is:

$$j = a\sigma \left[\left(V_D + V\right) 8 \pi e \frac{N}{k}\right]^{1/2} \exp\left(\frac{-eV_D}{KT}\right) \left[1 - \exp\left(\frac{-eV}{KT}\right)\right] \quad (9)$$

where σ is the semiconductor bulk conductivity.

The above equations will now be modified for the image force and tunnel effect corrections. As before, equations (8) and (9) for reverse voltages greater than about 0.5 volts are closely approximated by,

$$j = a\sigma \left(\frac{V_D + V}{\lambda_o}\right) \exp\left(\frac{-eV_D}{KT}\right) \text{ for a Mott Barrier, and} \quad (10)$$

$$j = a\sigma \left[\left(V_D + V\right) 8 \pi e \frac{N}{k}\right]^{1/2} \exp\left(\frac{-eV_D}{KT}\right) \quad (11)$$

for a Schottky Barrier, where the sign of j has been arbitrarily made positive.

As for the Diode Theory, the term $\exp\left(\frac{-eV_D}{KT}\right)$ is the factor most affected by the diminution of the barrier height due to the image force and tunnel penetration. Thus, eV_D will now be replaced by $eV_D - \Delta\phi$, where the $\Delta\phi$'s are the same correction factors used for the Diode Theory. Equations (10) and (11), when thus corrected, yield:

For a Mott Barrier with tunnel effect correction,

$$j = a\sigma \left(\frac{V_D + V}{\lambda_o}\right) \exp\left(\frac{-eV_D}{KT}\right) \exp\left[\frac{ex_c\left(V_D + V\right)}{\lambda_o KT}\right] \quad (12)$$

For a Schottky Barrier with tunnel effect correction,

$$j = a\sigma\left[\frac{(V_D+V)\,8\pi Ne}{k}\right]^{1/2} \exp\left(\frac{-eV_D}{KT}\right) \exp\left\{\left[\frac{(V_D+V)\,8\pi Ne^3}{}\right]^{1/2} \cdot \frac{x_c}{KT}\right\}. \quad (13)$$

For a Mott Barrier with image force correction,

$$j = a\sigma\left(\frac{V_D + V}{\lambda_o}\right) \exp\left(\frac{-eV_D}{KT}\right) \exp\left\{\left[\frac{e^3(V_D + V)}{\lambda_o\, k}\right]^{1/2} \cdot \frac{1}{KT}\right\} \cdot \quad (14)$$

For a Schottky Barrier with image force correction,

$$j = a\sigma\left[\frac{(V_D+V)\,8\pi Ne}{k}\right]^{1/2} \exp\left(\frac{-eV_D}{KT}\right) \exp \frac{\left[(V_D+V)\,e^7\pi N/2k^3\right]^{1/4}}{KT} \quad (15)$$

Equations (12), (13), (14), and (15) are the Diffusion Theory relations used in the reverse direction curve fitting in Chapter VI.

CHAPTER V

DIODE FORWARD DIRECTION CURVE FITTING

In this chapter, the experimental diode forward direction volt ampere characteristcs are fitted to the theoretical (forward direction) functional form, $I = A\left[e^{\alpha(V-IR)} -1\right]$. The resultant fit of the assumed functional form to the experimental data indicates with high confidence that the rectification characteristic is accurately described by the fitted relation which results:

$$I = 1.096 \times 10^{-8} \left[e^{12.39(V - 338.8I)} - 1\right].$$

The diode empirical volt ampere characteristics were taken from diodes which were made from the same material and in the same manner as the diodes used in the test for injection of minority carrier into the bulk material (see Chapters II and III). This should give assurance that the injection test results may be applied to the diodes under analysis.

Diode empirical volt ampere characteristics are listed in Table I. All of the analysis and curve fitting is based on the first four characteristics tabulated, which are typical for reduced TiO_2 point contact diodes. The high degree of consistency of the characteristics for the four diodes was achieved by using the same point contact and restricted contact placement region on one cleaved surface crystal for all of the diodes. Additionally, the diode V-I characteristics were displayed on an oscilloscope while contact adjustment was being made. In this fashion, it was possible to make contact adjustments which resulted in very consistent diode characteristics. Because of this, and the goodness of fit

which resulted, it was felt that the numerical constants determined by the curve fitting have considerable accuracy and are unique.

which resulted, it was felt that the numerical constants determined by the curve fitting have considerable accuracy and are unique.

	Diode I		Diode II		Diode III		Diode IV		Diode Average	
i	$I\cdot 10^{+6}$	V	$I\cdot 10^{+6}$	V	$I\cdot 10^{+6}$	V	$I\cdot 10^{+6}$	V	$I_i\cdot 10^{+6}$	V_i
1	-1	-2.05	-1	-3.6	-1	-3.9	-1	-4.3	-1	-3.4625
2	-2	-3.2	-2	-4.9	-2	-5.7	-2	-5.7	-2	-4.875
3	-3	-4.0	-3	-6.0	-3	-7.1	-3	-6.7	-3	-5.95
4	-4	-6.0	-4	-6.75	-4	-8.0	-4	-7.8	-4	-7.1375
5	+1.5	+0.45	+1.5	+0.4	+1.5	+0.5	+1.5	+0.3	+1.5	+0.4125
6	+10	+0.60	+10	+0.5	+10	+0.6	+10	+0.5	+10	+0.55
7	+20	+0.65	+20	+0.55	+20	+0.65	+20	+0.55	+20	+0.6
8	+100	+0.8	+100	+0.75	+100	+0.8	+100	+0.7	+100	+0.7625
9	+400	+1.0	+400	+1.0	+400	+0.95	+400	+0.95	+400	+0.975
10	+1000	+1.3	+1000	+1.3	+1000	+1.25	+1000	+1.20	+1000	+1.2625
11	+2000	+1.7	+2000	+1.7	+2000	+1.7	+2000	+1.65	+2000	+1.6875
12	+3000	+2.05	+3000	+2.0	+3000	+2.05	+3000	+2.00	+3000	+2.025
13	+4000	+2.4	+4000	+2.35	+4000	+2.4	+4000	+2.35	+4000	+2.375

TABLE I

DIODE CHARACTERISTICS DATA

Voltage reading in volts
Current reading in amperes

To smooth out what small variations existed among the four diodes, a diode average is presented in the last column of Table I. This diode average is the simple arithmetic mean voltage for each of the common current levels. These diode averages, $\left[I_i, V_i\right]$, are the statistics used in the curve fitting process.

The technique used for fitting the data to the theoretical model was that the sum of the squares of the voltage error between the fitted curve and that observed be minimized. For this type of fit, an explicit representation of one variable as a function of the other variable is required. The algebraic manipulation of $I = A\left[e^{\alpha(V-IR)} - 1\right]$ to the form $V = IR + \frac{1}{\alpha} \ln \frac{I + A}{A}$, satisfies this requirement.

In the following analysis, the symbols defined below will be used:

V = The theoretical applied voltage;

V_i = The observed average value of applied voltage when current I_i is flowing;

I = The theoretical current flowing when the applied voltage is V;

I_i = The observed current flowing when the applied voltage is V_i;

ϵ_i = The error between the theoretical applied voltage and the observed voltage when current I_i is flowing;

L = The error function which is to be minimized.

Using the above definitions, $\epsilon_i = RI_i + \frac{1}{\alpha} \ln \frac{I_i+A}{A} - V_i$. Hence, as described in the text, the function to be minimized is $L = \sum \epsilon_i^2$, where the summation is carried out over all

the positive values of I_i and V_i tabulated in Table I. Hence, L may be written as

$$L = \sum_{5}^{13} \left[RI_i + \frac{1}{\alpha} \ln \frac{I_i + A}{A} - V_i \right]^2 . \qquad (1)$$

Values of R, α, and A must now be found which yield the minimum value for L. This is accomplished by setting the partial derivatives of L with respect to R, α, and A equal to zero and solving the resulting equations simultaneously. The solution of these equations yields values (R_o, α_o, and A_o) for R, α, and A which result in a minimum value for L. Trivial solutions which result in maximization of L are discarded.

The simultaneous equations to be solved are:

$$\frac{\partial L}{\partial \lambda} = 2 \sum_{5}^{13} \epsilon_i \frac{\partial \epsilon_i}{\partial \lambda} = 0, \text{ where } \lambda = \alpha, A, R.$$

Now: $$\frac{\partial \epsilon_i}{\partial \alpha} = - \frac{1}{\alpha^2} \ln \frac{I_i + A}{A}, \quad \frac{\partial \epsilon_i}{\partial A} = \frac{-1}{\alpha A} \cdot \frac{I_i}{I_i + A},$$

$$\text{and} \quad \frac{\partial \epsilon_i}{\partial R} = I_i .$$

Hence,

$$\frac{\partial L}{\partial \lambda} = 2 \sum_{5}^{13} \epsilon_i \cdot \frac{-1}{\alpha^2} \ln \frac{I_i + A}{A},$$

$$\frac{\partial L}{\partial A} = 2 \sum_{5}^{13} \epsilon_i \cdot \frac{-1}{\alpha A} \cdot \frac{I_i}{I_i + A}, \text{ and}$$

the positive values of I_i and V_i tabulated in Table I.
Hence, L may be written as

$$L = \sum_{5}^{13}\left(RI_i + \frac{1}{\alpha}\ln\frac{I_i + A}{A} - V_i\right)^2 . \qquad (1)$$

Values of R, α, and A must now be found which yield the minimum value for L. This is accomplished by setting the partial derivatives of L with respect to R, α, and A equal to zero and solving the resulting equations simultaneously. The solution of these equations yields values (R_o, α_o, and A_o) for R, α, and A which result in a minimum value for L. Trivial solutions which result in maximization of L are discarded.

The simultaneous equations to be solved are:

$$\frac{\partial L}{\partial \lambda} = 2\sum_{5}^{13} \epsilon_i \frac{\partial \epsilon_i}{\partial \lambda} = 0, \text{ where } \lambda = \alpha, A, R.$$

Now: $\dfrac{\partial \epsilon_i}{\partial \alpha} = -\dfrac{1}{\alpha^2}\ln\dfrac{I_i + A}{A}$, $\dfrac{\partial \epsilon_i}{\partial A} = \dfrac{-1}{\alpha A}\cdot\dfrac{I_i}{I_i + A}$,

and $\dfrac{\partial \epsilon_i}{\partial R} = I_i$.

Hence,

$$\frac{\partial L}{\partial \lambda} = 2\sum_{5}^{13} \epsilon_i \cdot \frac{-1}{\alpha^2}\ln\frac{I_i + A}{A},$$

$$\frac{\partial L}{\partial A} = 2\sum_{5}^{13} \epsilon_i \cdot \frac{-1}{\alpha A}\cdot\frac{I_i}{I_i + A}, \text{ and}$$

$\frac{\partial L}{\partial R} = 2 \sum_{5}^{13} \epsilon_i I_i$. These partial derivatives are now set equal to zero and the constant non-zero multiplying factors divided out:

$$\frac{\partial L}{\partial \alpha} = \sum_{5}^{13} \left(RI_i + \frac{1}{\alpha} \ln \frac{I_i+A}{A} - V_i\right) \ln \frac{I_i + A}{A} = 0,$$

$$\frac{\partial L}{\partial A} = \sum_{5}^{13} \left(RI_i + \frac{1}{\alpha} \ln \frac{I_i + A}{A} - V_i\right) \frac{I_i}{I_i+A} = 0, \text{ and}$$

$$\frac{\partial L}{\partial R} = \sum_{5}^{13} \left(RI_i + \frac{1}{\alpha} \ln \frac{I_i + A}{A} - V_i\right) I_i = 0.$$

Rewriting to a more convenient form yields,

$$\sum_{5}^{13} (V_i - RI_i) \ln \frac{I_i + A}{A} = \frac{1}{\alpha} \sum_{5}^{13} \left(\ln \frac{I_i + A}{A}\right)^2. \tag{2}$$

$$\sum_{5}^{13} \left(V_i - RI_i\right) \frac{I_i}{I_i+A} = \frac{1}{\alpha} \sum_{5}^{13} \frac{I_i}{I_i + A} \ln \frac{I_i + A}{A}. \tag{3}$$

and

$$R \sum_{5}^{13} I_i^2 = \sum_{5}^{13} I_i V_i - \frac{1}{\alpha} \sum_{5}^{13} I_i \ln \frac{I_i + A}{A} \tag{4}$$

The values α_o, A_o, and R_o which satisfy equations (2), (3) and (4) result in a minimum value for L. Direct simultaneous solution of these equations by trial and error is possible but impractical. Hence, an iterative process type of solution using trial and error is made which leads fairly directly to the required solutions. This is done as follows: Simultaneous

solution of (2) and (3) is determined by trial and error with a value for R assumed. The values of α and A which result are then used in (4) where a direct computation of R may be made. This value of R is then used in the simultaneous solution of (2) and (3) once more. Again, the computed values of α and A are used to compute a value of R. This iterative process is continued until convergence to the desired degree of accuracy is achieved.

Simultaneous solution of (1) and (2) is achieved by the elimination of α . The resulting equation to be solved for A is:

$$\frac{\left[\sum_{5}^{13} (V_i - RI_i) \ln \frac{I_i + A}{A}\right]\left[\sum_{5}^{13} \frac{I_i}{I_i + A} \ln \frac{I_i + A}{A}\right]}{\left[\sum_{5}^{13} (V_i - RI_i) \frac{I_i}{I_i + A}\right]\left[\sum_{5}^{13} \left(\ln \frac{I_i + A}{A}\right)^2\right]} = 1 \quad (5)$$

This value of A (for an assumed value for R) is then used in equations (2) or (3) to calculate the value of α . R is then calculated from equation (4) using the previous solutions to (2) and (3), i.e.,

$$R = \frac{\sum_{5}^{13} I_i V_i - \frac{1}{\alpha} \sum_{5}^{13} I_i \ln \frac{I_i + A}{A}}{\sum_{5}^{13} I_i^2} \quad (6)$$

Cyclic use of the solutions to equations (5), (2) or (3), and (6) result in the parameter values (accurate to the indicated places):

$R_o \doteq 338.8$ ohms, $\alpha_o \doteq 12.39$ volts^{-1}, and $A_o \doteq 1.096 \times 10^{-8}$ amperes.

Hence, the diode forward direction fit is given by:

$$I = 1.096 \times 10^{-8} \left[e^{12.39 (V - 338.8 I)} - 1 \right] \text{ (amperes)}. \quad (7)$$

Visual indication of the accuracy of this fit is presented in Figure I. In this figure, the observed and calculated values of voltage are plotted for the fixed observed current levels. Additionally, the ϵ_i associated with each data point is indicated.

Also indicative of the goodness of the fit are the small values of the statistics L and max. $|\epsilon_i|$. There, calculated values are $L \doteq 0.001744$ and max. $|\epsilon_i| \doteq 0.032$.

FIGURE I

DIODE FORWARD DIRECTION CHARACTERISTIC

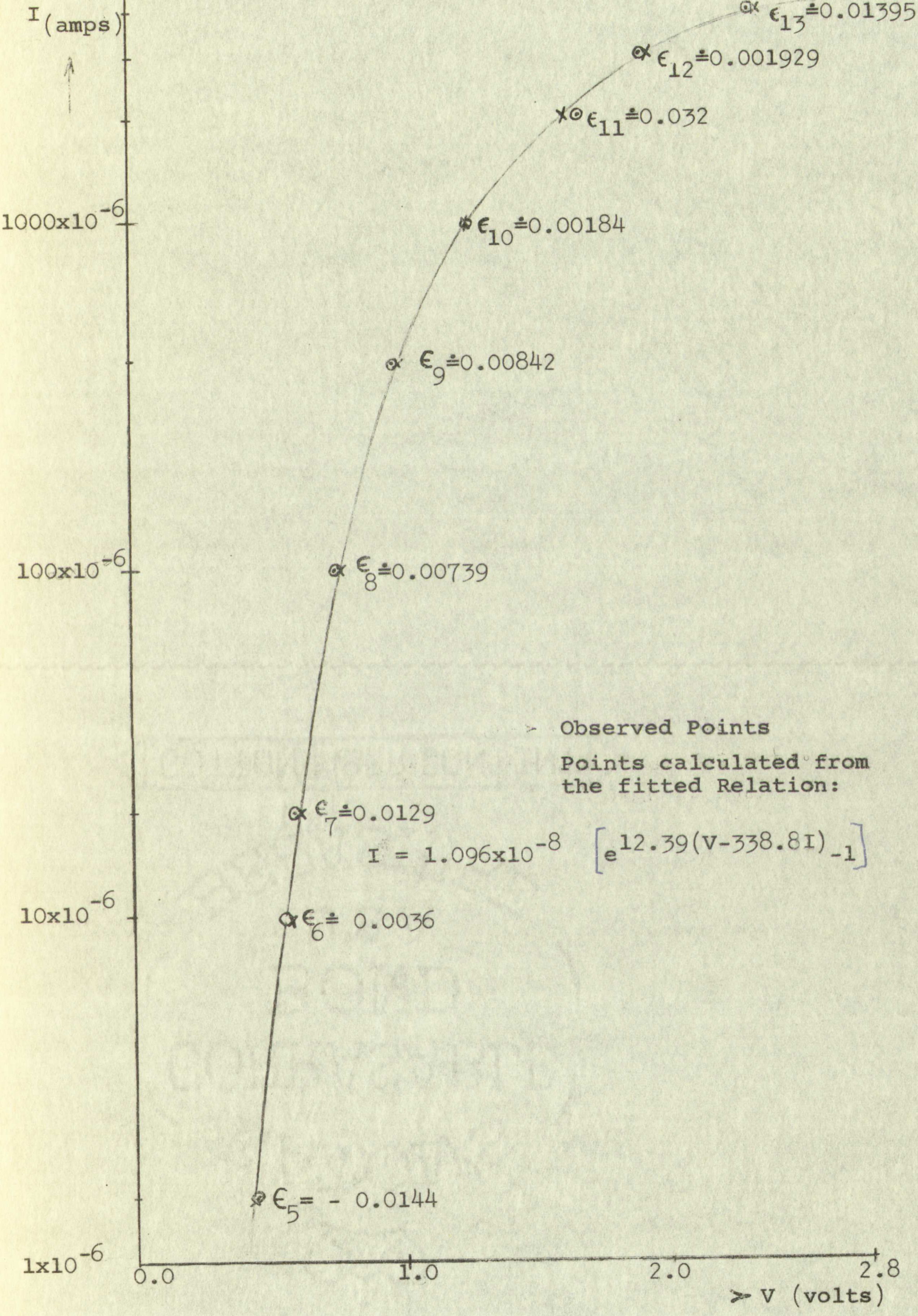

CHAPTER VI

DIODE REVERSE DIRECTION CURVE FITTING

The diode reverse direction equations which were partially derived in Chapter IV are fitted to the empirical data in this chapter. In all cases, the criterion for fitting is that the sum of the squares of the errors between the calculated current and the observed current be minimized. The details involved in the fitting have been omitted, as the forward direction fit of Chapter V is given in detail as an illustration of the method.

All of the equations for the Diode Theory and the Diffusion Theory are analyzed for the assumption of both Schottky and Mott Barriers and with correction for both the image force and the tunnel effect. Additonally, certain special functional forms of interest (as described later) are fitted.

In general, the theoretical equations are of the form $j = f(V)$ where j is the theoretical absolute value of the negative reverse current which flows when reverse voltage V is applied. Note that V is also a positive quantity for the equations derived. Hence, the ordered pairs of data $\left[V_i, I_i\right]$ in the reverse direction must also be taken as positive quantities, i.e., the absolute values. Therefore, the $\left[V_i, I_i\right]$ used are the magnitudes of the diode averages in Table I of Chapter V for i = 1, 2, 3, 4, (after conversion to statvolts and statamperes).

The general nomenclature and approach used is as follows:

$$L = \sum_{i=1}^{4} \epsilon_i^2$$ is the error function which is to be minimized,

where $$\epsilon_i = j\Big|_{V=V_i} - I_i.$$

The partial derivatives of L with respect to the adjusting parameters are set equal to zero and the resulting equations solved.

One general type of fit which was made several times will now be derived. This fit is the determination of the magnitude multiplying factor, γ , which will minimize L for some function $j = \gamma f(V)$. If the computed value of γ is close to one, then the function f (V) does not need a γ correction multiplier. The value of γ is computed as follows:

Let $\bar{j} = \gamma f(V) = \gamma j$, where $j = f(V)$.

Then $\epsilon_i = \gamma j_i - I_i$ and $L = \sum (\gamma j_i - I_i)^2$

Thus, $\frac{\partial L}{\partial \gamma} = 2 \sum \epsilon_i \frac{\partial \epsilon_i}{\partial \gamma} = 2 \sum \left(\gamma j_i - I_i\right) j_i$, or

$$\gamma = \frac{\sum j_i I_i}{\sum j_i^2}$$ is the equation to be solved.

Hence, a "Check γ" is the γ calculated for some function which has already been fitted with respect to parameters other than the magnitude coefficient. Repeating, if the γ thus computed is close to unity, little decrease in the value of L is achievable by adjusting the magnitude coefficient.

The values of the numerical constants involved in the calculations are tabulated in Appendix I.

A. - General Diode Theory Fit

In general, all of the Diode Theory equations are of the functional form, $j = A \exp\left[\gamma\left(V_D + V\right)^u\right]$. Before beginning the fitting for each Diode Theory equation, it would be useful to know the best fit of the Diode Theory functional form to the data which is possible. This is accomplished by fitting the parameters γ and u, in $j = A \exp\left[\gamma\left(V_D + V\right)^u\right]$, as follows:

Make the transformations,

$x = \ln \gamma$, $Y = \ln(\ln j)$, and $Z_i = \ln\left[\ln \frac{I_i}{A}\right]$.

Then $E = \sum_1^4 \left[x + u \ln\left(V_D + V_i\right) - Z_i\right]^2$. Setting $\frac{\partial E}{\partial x} = 0$,

and $\frac{\partial E}{\partial u} = 0$, yields the two simultaneous equations to be solved:

$$\sum_1^4 \left[x + u \ln\left(V_D + V_i\right)\right] = \sum_1^4 Z_i, \text{ and} \qquad (1)$$

$$\sum_1^4 \left[x + u \ln\left(V_D + V_i\right)\right] \ln\left(V_D + V_i\right) = \sum_1^4 Z_i \ln\left(V_D + V_i\right) \qquad (2)$$

The solutions to (1) and (2) are

$u \doteq 0.42146$ and $\gamma \doteq 27.894$. The fit which results yields $L \doteq 0.9845 \times 10^6$ and check $\gamma \doteq 0.98056$.

Since γ is so close to unity, $L \doteq 0.9845 \times 10^6$ is very close to the absolute minimum L which could be achieved using the Diode Theory.

In the Diode Theory fitting which follows, the different particular equation fitting is achieved using the general equation (1).

B - Diode Theory Equation for a Schottky Barrier with Image Force Correction

$$j = A \exp \left\{ \left[(V_D + V) e^7 \pi \frac{N}{2k^3} \right]^{1/4} \cdot \frac{1}{KT} \right\} \text{ or}$$

$$j = A \exp \left[\Delta (V_D + V)^{1/4} \right] \text{ where } \tau = \Delta \doteq 6.846 \text{ and } u = 0.25.$$

$$L = \sum_1^4 \epsilon_i^2 \doteq 243 \times 10^6 \text{ for no corrections at all.}$$

$$\text{Check } \gamma = \frac{\sum_1^4 j_i I_i}{\sum_1^4 j_i^2} \doteq 1.83. \text{ Hence, a magnitude}$$

correction would be helpful and

$$\bar{L} \doteq 14.85 \times 10^6 \text{ for a } \gamma = 1.83 \text{ correction.}$$

It is desirable to know how much the fit can be improved by an adjustment of the coefficient in the exponential term. Thus, let $j = A \exp \left[\tau (V_D + V)^{1/4} \right]$ and determine the value of τ which will minimize L, where $\tau \doteq 6.846$ v. Using equation (1), the equation to be solved is:

$$\sum_1^4 \left[\ln(6.846v) + 0.25 \ln \left(V_D + V_i \right) \right] = \sum_1^4 z_i. \text{ The}$$

solution is, $v \doteq 2.07$. Using this value,

$L \doteq 8.892 \times 10^6$ and check $\gamma \doteq 1.14$.

C - Diode Theory Equation for a Schottky Barrier With Tunnel Effect Correction

$$j = A \exp \left\{ \left[(V_D + V)\ 8 e^3 \pi \frac{N}{k} \right]^{1/2} \cdot \frac{x_c}{KT} \right\} \text{or}$$

In the Diode Theory fitting which follows, the different particular equation fitting is achieved using the general equation (1).

B - Diode Theory Equation for a Schottky Barrier with Image Force Correction

$$j = A \exp\left\{\left[(V_D + V)\, e^7 \pi \frac{N}{2K^3}\right]^{1/4} \cdot \frac{1}{KT}\right\} \text{ or}$$

$$j = A \exp\left[\Delta (V_D + V)^{1/4}\right] \text{ where } \Upsilon = \Delta \doteq 6.846 \text{ and } u = 0.25.$$

$$L = \sum_1^4 \epsilon_i^2 \doteq 243 \times 10^6 \text{ for no corrections at all.}$$

$$\text{Check } \gamma = \frac{\sum_1^4 j_i I_i}{\sum_1^4 j_i^2} \doteq 1.83.$$ Hence, a magnitude correction would be helpful and

$L \doteq 14.85 \times 10^6$ for a $\gamma = 1.83$ correction.

It is desirable to know how much the fit can be improved by an adjustment of the coefficient in the exponential term. Thus, let $j = A \exp\left[\Upsilon (V_D + V)^{1/4}\right]$ and determine the value of Υ which will minimize L, where $\Upsilon \doteq 6.846$ v. Using equation (1), the equation to be solved is:

$$\sum_1^4 \left[\ln(6.846v) + 0.25 \ln(V_D + V_i)\right] = \sum_1^4 z_i.$$ The solution is, $v \doteq 2.07$. Using this value, $L \doteq 8.892 \times 10^6$ and check $\gamma \doteq 1.14$.

C - Diode Theory Equation for a Schottky Barrier With Tunnel Effect Correction

$$j = A \exp\left\{\left[(V_D + V)\, 8 e^3 \pi \frac{N}{K}\right]^{1/2} \cdot \frac{x_c}{KT}\right\} \text{ or}$$

$$j = A \exp\left[\Delta x_c \left(V_D + V\right)^{1/2}\right], \text{ where}$$

$$u = 0.5 \text{ and } \gamma = x_c \frac{\left(8 e^3 \pi \frac{N}{k}\right)^{1/2}}{KT} \doteq 4.05 \cdot 10^{10} x_c.$$

Using equation (1), the value of x_c for minimum L is found from the solution of:

$$\sum_1^4 \left[\ln\left(4.05 \cdot 10^{10} x_c\right) + 0.5 \ln\left(V_D + V_i\right)\right] = \sum_1^4 Z_i.$$

$x_c \doteq 9.2 \cdot 10^{-10}$ (cm) is the solution and for this fit,

$L \doteq 3.105 \times 10^6$ and check $\gamma \doteq 1.0097$.

D - Diode Theory Equation for a Mott Barrier With Image Force Correction

$$j = A \exp\left\{\left[e^3\left(V_D + V\right)\frac{1}{k\lambda_o}\right]^{1/2} \cdot \frac{1}{KT}\right\} \text{ or}$$

$$j \doteq A \exp\left[\Delta \lambda_o^{-1/2}\left(V_D + V\right)^{1/2}\right], \text{ where}$$

$u = 0.5$ and $\gamma = e^{3/2}\, k^{-1/2} (KT)^{-1}\, \lambda_o^{-1/2} \doteq 2.332 \times 10^{-2} \lambda_o^{-1/2}$.

Using equation (1), the value of λ_o for minimum L is found from the solution of:

$$\sum_1^4 \left[\ln\left(2.332 \times 10^{-2} \lambda_o^{-1/2}\right) + 0.5 \ln\left(V_D + V_i\right)\right] = \sum_1^4 Z_i.$$

$\lambda_o \doteq 3.9 \times 10^{-7}$ cm is the solution, and for this fit,

$L \doteq 3.105 \times 10^6$ and check $\gamma \doteq 1.0097$.

E - Diode Theory Equation for a Mott Barrier With Tunnel Effect Correction

$$j = A \exp \left\{ \left[e\left(V_D + V\right) \frac{x_c}{\lambda_o} \right] \cdot \frac{1}{KT} \right\} \text{ or}$$

$$j = A \exp \left[\Delta\beta \left(V_D + V \right) \right], \text{ where}$$

$$u = 1.0,\ r = \frac{e}{KT}\beta \doteq 1.174 \times 10^4\ \beta, \text{ and } \beta = \frac{x_c}{\lambda_o}\ .$$

Using equation (1), the value of β for minimum L is found from the solution of:

$$\sum_1^4 \left[\ln(1.175 \times 10^4 \beta) + 1.0 \ln\left(V_D + V_i\right) \right] = \sum_1^4 Z_i .$$

$\beta = \frac{x_c}{\lambda_o} \doteq 2 \times 10^{-2}$ is the solution and for this fit,

$L \doteq 34.06 \times 10^6$ and check $\gamma \doteq 1.04$.

F - Diffusion Theory Equation for a Schottky Barrier With Image Force Correction

Because of the possible inaccuracy of the values of σ and a, all of the Diffusion Theory equations will be fitted with respect to the outside magnitude factor using the symbol γ for the correction.

In the first equation considered, a Schottky Barrier with image force corrections, no fitting is required other than the γ magnitude factor:

$$j = a\sigma \left[\frac{\left(V_D + V\right) 8\pi eN}{k} \right]^{1/2} \exp\left(\frac{-eV_D}{KT} \right) \exp\left\{ \frac{\left[\left(V_D + V\right) e^7 \pi N / 2k^3\right]^{1/4}}{KT} \right\}, \text{ or}$$

$$j = \Delta\left(V_D + V\right)^{1/2} \exp\left[M\left(V_D + V\right)^{1/4}\right], \text{ where}$$

$$\Delta = a\sigma\left(\frac{8\pi Ne}{k}\right)^{1/2} \exp \frac{-e\,V_D}{KT} \doteq 1.527 \times 10^3, \text{ and}$$

$$M = \frac{\left(e^7\,\pi N/2k^3\right)^{1/4}}{KT} \doteq 6.846. \text{ Upon calculation,}$$

$L \doteq 114.9 \times 10^6$ for no correction, i.e., $\gamma = 1$.

$$\gamma = \frac{\sum_1^4 I_i j_i}{\sum_1^4 (j_i)^2} = 2.773. \text{ The use of this } \gamma \text{ in } \bar{j} =$$

γj yields an $\bar{L} \doteq 7.65 \times 10^6$.

G - Diffusion Theory Equation for a Schottky Barrier With Tunnel Effect Correction

$$j = \gamma a\sigma \left[\frac{\left(V_D+V\right)8\pi Ne}{k}\right]^{1/2} \exp\left(\frac{-eV_D}{KT}\right)\exp\left\{\left[\frac{\left(V_D+V\right)8\pi Ne}{k}\right]^{1/2} \cdot \frac{ex_c}{KT}\right\}$$

$$\text{or } j = \gamma\,\Delta\left(V_D + V\right)^{1/2} \exp\left[DX_c\left(V_D + V\right)\right], \text{ where}$$

$$\Delta = a\sigma\left(\frac{8\pi Ne}{k}\right)^{1/2} \exp\left(\frac{-eV_D}{KT}\right) \doteq 1.527 \times 10^3, \text{ and}$$

$$D = \left(\frac{8\pi Ne}{k}\right)^{1/2} \cdot \frac{e}{KT} \doteq 4.05 \times 10^9.$$

$\frac{\partial L}{\partial x_c} = 0$, yields one equation:

$$\gamma\Delta \sum_1^4 \left(V_D+V_i\right)^{3/2}\left\{\exp\left[DX_c\left(V_D+V_i\right)^{1/2}\right]\right\}^2 =$$

$$\sum_1^4 I_i\left(V_D + V_i\right) \exp\left[DX_c\left(V_D + V_i\right)^{1/2}\right].$$

$\frac{\partial L}{\partial \gamma} = 0$, yields another equation:

$$\gamma \Delta \sum_{1}^{4} \left(V_D + V_i\right) \left\{ \exp\left[DX_c \left(V_D + V_i\right)^{1/2} \right] \right\}^2 =$$

$$\sum_{1}^{4} I_i \left(V_D + V_i\right)^{1/2} \exp\left[DX_c \left(V_D + V_i\right)^{1/2} \right] .$$

γ may be eliminated between the two equations to yield one equation to be solved for one unknown, x_c:

$$\frac{\sum_{1}^{4} \left(V_D + V_i\right)^{3/2} \left\{ \exp\left[Dx_c \left(V_D + V_i\right)^{1/2} \right] \right\}^2}{\sum_{1}^{4} \left(V_D + V_i\right) \left\{ \exp\left[Dx_c \left(V_D + V_i\right)^{1/2} \right] \right\}^2} \times$$

$$\frac{\sum_{1}^{4} I_i \left(V_D + V_i\right)^{1/2} \exp\left[Dx_c \left(V_D + V_i\right)^{1/2} \right]}{\sum_{1}^{4} I_i \left(V_D + V_i\right) \exp\left[Dx_c \left(V_D + V_i\right)^{1/2} \right]} = 1$$

The solutions to the above equations are

$x_c \doteq 5.35 \times 10^{-9}$ (cm) and $\gamma \doteq 1.5445$ and the resulting fit yields $L \doteq 0.4474 \times 10^6$.

H - <u>Diffusion Theory Equation for a Mott Barrier With Image Force Corrections</u>

$$j = \gamma a \sigma \left(\frac{V_D + V}{\lambda_o}\right) \exp\left(\frac{-eV_D}{KT}\right) \exp\left\{ \left[\frac{e^3 \left(V_D + V\right)}{\lambda_o \, k}\right]^{1/2} \cdot \frac{1}{KT} \right\} \text{ or}$$

$$j = \gamma \Delta \left(V_D + V\right) \frac{1}{\lambda_o} \exp \left[M \lambda_o^{-1/2} \left(V_D + V\right)^{1/2}\right], \text{ where}$$

$$\Delta = a\sigma \exp\left(\frac{-eV_D}{KT}\right) \doteq 4.43 \times 10^{-3}, \text{ and}$$

$$M = e^{3/2} k^{-1/2} (KT)^{-1} \doteq 2.332 \times 10^{-2}.$$

$\dfrac{\partial L}{\partial \lambda_o} = 0$, yields one equation:

$$\frac{\gamma \Delta}{\lambda_o} \sum_1^4 \left(V_D + V_i\right)^2 \left[\frac{2}{M} \lambda_o^{1/2} + \left(V_D + V_i\right)^{1/2}\right] \left\{ \exp\left[M \lambda_o^{-1/2} \left(V_D + V_i\right)^{1/2}\right] \right\}^2 =$$

$$\sum_1^4 I_i \left(V_D + V_i\right) \left[\frac{2}{M} \lambda_o^{1/2} + \left(V_D + V_i\right)^{1/2}\right] \exp\left[M \lambda_o^{-1/2} \left(V_D + V_i\right)^{1/2}\right].$$

$\dfrac{\partial L}{\partial \gamma} = 0$, yields another equation:

$$\frac{\gamma \Delta}{\lambda_o} \sum_1^4 \left(V_D + V_i\right)^2 \left\{\exp\left[M \lambda_o^{-1/2} \left(V_D + V_i\right)^{1/2}\right]\right\}^2 =$$

$$\sum_1^4 I_i \left(V_D + V_i\right) \exp\left[M \lambda_o^{1/2} \left(V_D + V_i\right)^{1/2}\right]$$

γ may be eliminated between the two equations to yield one equation to be solved for one unknown, λ_o:

$$\frac{\sum_{1}^{4}(V_D+V_i)^2\left[\frac{2}{M}\lambda_o^{1/2}+(V_D+V_i)^{1/2}\right]\left\{\exp\left[M\lambda_o^{-1/2}(V_D+V_i)^{1/2}\right]\right\}^2}{\sum_{1}^{4}(V_D+V_i)^2\left\{\exp\left[M\lambda_o^{-1/2}(V_D+V_i)^{1/2}\right]\right\}^2}\ \mathrm{x}$$

$$\frac{\sum_{1}^{4} I_i\,(V_D+V_i)\exp\left[M\lambda_o^{-1/2}(V_D+V_i)^{1/2}\right]}{\sum_{1}^{4} I_i\,(V_D+V_i)\left[\frac{2}{M}\lambda_o^{-1/2}+(V_D+V_i)^{1/2}\right]\exp\left[M\lambda_o^{-1/2}(V_D+V_i)^{1/2}\right]}=1$$

The solutions to the above equations are $\lambda_o \doteq 2.55 \times 10^{-6}$ (cm) and $\gamma \doteq 26.22$ and the resulting fit yields $L \doteq 0.36075 \times 10^6$.

I - Diffusion Theory Equation for a Mott Barrier With Tunnel Effect Correction

$$j = a\sigma \left(V_D+V\right) \frac{1}{\lambda_o} \exp\left[\frac{e\, Vx_c - e\, V_D\left(\lambda_o - x_c\right)}{\lambda_o KT}\right], \text{ or}$$

$$j = a\sigma \left(V_D+V\right) \frac{1}{\lambda_o} \exp\left(\frac{-e\, V_D}{KT}\right) \exp\left[\frac{e\, x_c\left(V_D+V\right)}{\lambda_o KT}\right].$$

Let $\beta = \frac{x_c}{\lambda_o}$, $x_o = \frac{x_c}{\gamma}$, $M = \frac{e}{KT} \doteq 1.175 \times 10^4$, and

$\Delta = a\sigma \exp\left(\frac{-e\, V_D}{KT}\right) \doteq 4.43 \times 10^{-3}$. Then

$j = \Delta\left(V_D+V\right) \frac{\beta}{x_o} \exp\left[M\beta\left(V_D+V\right)\right]$ is to be fitted to the data by optimizing the values of the parameters β and x_o. The association of β to the exponential makes β a constant as far as the outside magnitude factors are concerned. Thus, to be able to make the appropriate magnitude adjustment, the relation $x_o = \frac{x_c}{\gamma}$ was introduced.

$\frac{\partial L}{\partial \beta} = 0$, yields one equation:

$$\frac{\Delta\beta}{x_o} \sum_1^4 \left(V_D+V_i\right)^2\left(\frac{1}{M\beta} + V_D+V_i\right)\left\{\exp\left[M\left(V_D + V_i\right)\beta\right]\right\}^2 =$$

$$\sum_1^4 I_i \left(V_D + V_i\right)\left[\frac{1}{M\beta} + V_D + V_i\right] \exp\left[M\left(V_D + V_i\right)\beta\right].$$

$\frac{\partial L}{\partial x_o} = 0$, yields another equation:

$$\frac{\Delta\beta}{x_o} \sum_{1}^{4} \left(V_D+V_i\right)^2 \left\{ \exp\left[M\left(V_D+V_i\right)\beta\right] \right\}^2 = \sum_{1}^{4} I_i\left(V_D+V_i\right)\exp\left[M\left(V_D+V_i\right)\beta\right].$$

x_o may be eliminated between the two equations to yield one equation to be solved for one unknown, β:

$$\frac{\sum_{1}^{4} \left(V_D+V_i\right)^2 \left(\frac{1}{M\beta} + V_D+V_i\right) \left\{ \exp\left[M\beta\left(V_D+V_i\right)\right] \right\}^2}{\sum_{1}^{4} \left(V_D+V_i\right)^2 \left\{ \exp\left[M\beta\left(V_D+V_i\right)\right] \right\}^2} \times$$

$$\frac{\sum_{1}^{4} I_i \left(V_D+V_i\right) \exp\left[M\beta\left(V_D+V_i\right)\right]}{\sum_{1}^{4} I_i \left(V_D+V_i\right)\left[\frac{1}{M\beta} + V_D + V_i\right] \exp\left[M\beta\left(V_D+V_i\right)\right]} = 1$$

The solutions to the above equations are $\beta \doteq 4.275 \times 10^{-3}$ and $x_o \doteq 1.45 \times 10^{-10}$.

Hence,

$$x_c = \gamma\, x_o \doteq 1.45 \times 10^{-10}\, \gamma \text{ (cm) and } \lambda_o = \frac{\gamma x_o}{\beta} \doteq 3.39 \times 10^{-8} \text{(cm)},$$

where any value deemed appropriate may be assigned to γ . The fit which results yields $L \doteq 127.2 \times 10^6$.

CHAPTER VII

SUMMARY AND INTERPRETATION OF THE CURVE FITTING RESULTS

The evaluation of the fit of an observed phenomena to a fitted mathematical model involves two basic considerations:

1) How small is the value of the computed error function, $L = \sum \epsilon_i^2$, and

2) How reasonable are the values of the fitted parameters in light of the association of these parameters to the physical situation.

Additionally, if no γ magnitude correction parameter (see Chapter VI) has been fitted in the model, a "check γ" calculation indicates that the error in the fit is not due to the magnitude coefficient if the check γ is close to unity.

The forward direction fit of Chapter V was excellent and with the exception of the computed value of α, no deviations from the theoretical expectations occurred. The theory assigns a value to α of $\frac{e}{KT}$ or about 40 $(\text{volts})^{-1}$ at room temperature as compared to the fitted value of 12.39 $(\text{volts})^{-1}$. However, this value is not disturbing in light of the fact that analysis of a large number of the characteristics of both silicon and germanium diodes gave values of α ranging in value from 5 to 35 $(\text{volts})^{-1}$[1]. The value of A computed was 1.096×10^{-8} amperes. Using this value and the theoretical relationship,

---

[1] Torrey and Whitmer, Crystal Rectifiers.

CHAPTER VII

SUMMARY AND INTERPRETATION OF THE CURVE FITTING RESULTS

The evaluation of the fit of an observed phenomena to a fitted mathematical model involves two basic considerations:

1) How small is the value of the computed error function,

$$L = \sum_i \epsilon_i^2 \text{, and}$$

2) How reasonable are the values of the fitted parameters in light of the association of these parameters to the physical situation.

Additionally, if no γ magnitude correction parameter (see Chapter VI) has been fitted in the model, a "check γ" calculation indicates that the error in the fit is not due to the magnitude coefficient if the check γ is close to unity.

The forward direction fit of Chapter V was excellent and with the exception of the computed value of α, no deviations from the theoretical expectations occurred. The theory assigns a value to α of $\frac{e}{KT}$ or about 40 (volts)$^{-1}$ at room temperature as compared to the fitted value of 12.39 (volts)$^{-1}$. However, this value is not disturbing in light of the fact that analysis of a large number of the characteristics of both silicon and germanium diodes gave values of α ranging in value from 5 to 35 (volts)$^{-1}$ [1]. The value of A computed was 1.096×10^{-8} amperes. Using this value and the theoretical relationship,

---

[1] Torrey and Whitmer, Crystal Rectifiers.

$A = a\ n\ e \left(\frac{KT}{2\pi m^*}\right)^{1/2} \exp\left(\frac{-eV_D}{KT}\right)$, from Chapter IV, a value for the equilibrium barrier diffusion potential, V_D, was calculated. The value computed, $V_D \doteq 0.5884$ volts $\doteq$ 1.961×10^{-3} statvolts, was the value used for the reverse direction curve fitting.

The Diode Theory reverse direction fitting will now be discussed.

For the Schottky barrier with image force correction, the fit was poor for all adjustments made. L was 243×10^6 for no adjustments, 19.85×10^6 for a $\gamma \doteq 1.83$ correction, and 8.89×10^6 for a correction of the exponential coefficient.

The equations for the Schottky barrier with tunnel effect correction and the equation for the Mott barrier with image force correction are equivalent functional forms. Hence, for both fits, $L \doteq 3.105 \times 10^6$ and check $\gamma \doteq 1.0097$. The value of check γ indicates little improvement can be made by adjustment of the magnitude coefficient. The differences in the two fits lie in the computed values of the parameters: $x_c \doteq 9.2 \times 10^{-10}$ (cm) and $\lambda_o \doteq 4 \times 10^{-7}$ (cm). The value of x_c is considered unreasonably small and, hence, the tunnel effect corrected Schottky barrier is not considered appropriate. The value for the Mott barrier thickness, $\lambda_o \doteq 4 \times 10^{-7}$ (cm), is considered reasonable.

For the tunnel effect corrected Mott barrier, the computed L was 34.06×10^6 for $\beta = \frac{x_c}{\lambda_o} \doteq 2 \times 10^{-2}$. The resulting fit yielded a check $\gamma \doteq 1.04$. It is concluded that this modeldoes not fit the observed phenomena.

In summary, for the Diode Theory, the image force corrected Mott barrier equation most reasonably fits the experimental data. Further support of this conclusion is given by the value of u computed ($u \doteq 0.42$) for the general Diode Theory Fit which is close to the theoretically required value of $u = 0.5$ for the image force corrected Mott barrier.

The Diffusion Theory reverse direction fitting will now be discussed.

For the image force corrected Schottky barrier, the fit was poor, L being 115×10^{6} for no correction and 7.65×10^{6} for a $\gamma \doteq 2.773$ correction.

The fit of the tunnel effect corrected Schottky barrier yielded better results, L being 0.4474×10^{-6} for a dual fit of $x_c \doteq 5.35 \times 10^{-9}$ (cm) and $\gamma \doteq 1.545$. However, the value of x_c is considered to be too small to be reasonable.

The image force corrected Mott barrier equation yielded the best fit of all those considered. L was 0.36075×10^{6} for a dual fit of $\lambda_o \doteq 2.55 \times 10^{-6}$(cm) and $\gamma \doteq 26.22$. The value of λ_o is considered very reasonable and the value of γ is not considered unreasonably high in view of the possible errors in the values of the multiplying physical constants.

For the tunnel effect corrected Mott barrier, the resulting fit is outstandingly bad. For a dual fit of x_c and λ_o (which explicitly included a γ correction factor), the resulting L was 127.2×10^{6}.

In summary, in the reverse direction for both the Diode Theory and the Diffusion Theory, the image force corrected Mott barrier equations most reasonably describe the experimental data. The joint results indicate a Mott barrier thickness of

In summary, for the Diode Theory, the image force corrected Mott barrier equation most reasonably fits the experimental data. Further support of this conclusion is given by the value of u computed ($u \doteq 0.42$) for the general Diode Theory Fit which is close to the theoretically required value of $u = 0.5$ for the image force corrected Mott barrier.

The Diffusion Theory reverse direction fitting will now be discussed.

For the image force corrected Schottky barrier, the fit was poor, L being 115×10^{6} for no correction and 7.65×10^{6} for a $\gamma \doteq 2.773$ correction.

The fit of the tunnel effect corrected Schottky barrier yielded better results, L being 0.4474×10^{-6} for a dual fit of $x_c \doteq 5.35 \times 10^{-9}$ (cm) and $\gamma \doteq 1.545$. However, the value of x_c is considered to be too small to be reasonable.

The image force corrected Mott barrier equation yielded the best fit of all those considered. L was 0.36075×10^{6} for a dual fit of $\lambda_o \doteq 2.55 \times 10^{-6}$ (cm) and $\gamma \doteq 26.22$. The value of λ_o is considered very reasonable and the value of γ is not considered unreasonably high in view of the possible errors in the values of the multiplying physical constants.

For the tunnel effect corrected Mott barrier, the resulting fit is outstandingly bad. For a dual fit of x_c and λ_o (which explicitly included a γ correction factor), the resulting L was 127.2×10^{6}.

In summary, in the reverse direction for both the Diode Theory and the Diffusion Theory, the image force corrected Mott barrier equations most reasonably describe the experimental data. The joint results indicate a Mott barrier thickness of

$\lambda_o \doteq 10^{-6}$ (cm) and a barrier height of $V_D \doteq 0.58$ volts.

CHAPTER VIII

SUMMARY AND CONCLUSIONS

By exercising suitable precautions in the fabrication process, point contact diodes can be made utilizing reduced single crystal rutile TiO_2. The resulting diodes have characteristics which are sufficiently good for possible consideration as a future development item.

The development of a point contact transistor, using rutile, is not considered possible as no evidence of minority carrier injection was observed.

In the forward direction, the uncorrected Diode Theory functional form fits the data exceedingly well. In the reverse direction, the fitting process indicates (for both Diode and Diffusion Theory) that the rectification phenomenon is most likely attributable to a Mott type barrier in which the image forces reduce the effective barrier height in the reverse direction. The associated Mott barrier voltage and thickness which results is $V_D \doteq 0.58$ volts and $\lambda_o \doteq 10^{-6}$ (cm). Additional evidence which supports the existence of a Mott barrier as the rectification phenomena are:

1) In the test for contact injection (Chapter III), the value of $\frac{2\pi rV}{I}$ decreased with decreasing separation distances (r) between the rectifying and non-rectifying contacts. This decrease in resistivity, with decreasing values of r, is most likely due to the presence of a surface layer or film which has a higher value of resistivity than the bulk resistivity of the semiconductor. This is the type of non-uniform

impurity distribution required for a Mott barrier.

2) The existence of high resistivity surface films is plausible, considering the charge transport mechanism involving oxygen vacancy centers with associated free donor electrons. Hence, oxygen vacancy centers near the surface of the semiconductor may be slowly refilled by room temperature oxidation which would result in a higher surface resistivity.

The above considerations add weight to the conclusions of the theoretical-empirical analysis.

B I B L I O G R A P H Y

BIBLIOGRAPHY

1. Bardeen, John, "Surface States and Rectification at A Metal Semi-Conductor Contact," Phys. Rev., Vol. 71, 717-727, May 1947.

2. Brattain and Bardeen, J.,"Nature of the Forward Current in Germanium Point Contacts," Phys. Rev., 74, 231, 1948.

3. Breckenridge and Hosler, "Electrical Properties of Titanium Dioxide Semiconductors," Phys. Rev., Vol. 41, 793-803, August 1953.

4. Grant, F. A., Properties of Rutile (Titanium Dioxide), NBS Project No. 0900-11-4475, 1959.

5. Hollander and Castro, "Anisotropic Conduction in Non-stoichiometic Rutile," Phys. Rev., Vol. 119, 1882-1885, September 1960.

6. Hollander, Diesel, and Vick, "Piezoresistivity in the Oxide Semiconductor Rutile (TiO_2)," Phys. Rev., Vol. 117, 1469-1472, March 1960.

7. Kittel, Charles, Introduction to Solid State Physics, New York: John Wiley and Sons, Inc., 1953, 617 pp.

8. Komolova, T. I., and Nasledov, D. N., Radiotekhnike i eletronika, No. 6, 1033-1037, 1959.

9. Middlebrook, R. D., An Introduction to Junction Transistor Theory, John Wiley and Sons, Inc., 1957.

10. Shockley, William, Electrons and Holes in Semiconductors, D. Van Nostrand Company, Inc., 1950.

11. Sive, John N., The Properties, Physics, and Design of Semiconductor Devices, D. Van Nostrand Company, Inc., 1959.

12. Torrey and Whitmer, Crystal Rectifiers, McGraw-Hill, 1948.

A P P E N D I X

APPENDIX I

NUMERICAL CONSTANTS

In this appendix the various numerical constants which appear in the theoretical diode volt-ampere equations are tabulated for convenient reference. Additionally, the sources of the numbers are given along with comments on the type of averaging made to minimize the errors in the physical parameters not precisely known. All values are given in terms of Electrostatic Cgs Units. These units are sometimes given the prefix stat (such as statvolts) and are the result of using centimeters, grams, and seconds, and the assumption of unity capacity between two one-centimeter square plates with one centimeter of separation.

Symbol	Definition of Unit	Numerical Value	Information Source	Comments
m	Electronic (rest) mass in grams	9.038×10^{-28}	Ref. 1, p.274	
m*	Effective electron mass in grams	50 m or 4.519×10^{-26}	Table I of Ref. 2	$\frac{m^*}{m}$ ranges in value from 30 to 100. To minimize the error, an inverse square root average was taken.
e	Electronic charge in stat-coulombs	4.767×10^{-10}	p. 274 of Ref. 1	

Symbol	Definition of Unit	Numerical Value	Information Source	Comments
n	Concentration of free electrons per cm^3 at T = 294°K	3.7×10^{19}	Fig. 8 and Eq. (5) of Ref.2	n is calculated using Eq. (5) for R = 0.2 from interpolation in Fig. 8.
T	Temperature at which measurements were made in degrees Kelvin	294°K		
a	Approximation to the area of the blunt point contact of radius, r ≐ 0.004 cm.	$a = \pi r^2$ 5.02655×10^{-5}		
No symbol	Factor to convert amperes to statamperes	3×10^9	p.25 of Ref. 1)	
No symbol	Factor to convert volts to statvolts	$\frac{1}{300}$	p. 25 of Ref. 1)	
K	Boltzmann's constant in erg (°K^{-1})	1.38×10^{-16}	p. 3405 of Ref. 3)	
k	Dielectric constant	121	p.794 of Ref. 2)	For single crystals of rutile, the dielectric constant is 173 in the c direction and 89 in the a direction. To minimize the error, an inverse square root average was taken.

Symbol	Definition of Unit	Numerical Value	Information Source	Comments
σ	Bulk conductivity at 294°K for Linde single crystal rutile reduced 10 minutes at 800°C.	8.98×10^{11}	Fig. 7 of Ref. 2)	Interpolation in Fig. 7 was required.
N	Donor impurity concentration at 294 K in electrons per cm^3 for Linde single crystal rutile reduced 10 minutes at 800°C.	1.2×10^{21}	Table I of Ref. 2)	Interpolation in Table I was required.
V_D	Barrier diffusion voltage for the diodes under analysis as calculated in the text.	0.5884 volts or 1.961×10^{-3} statvolts		
λ_o	Thickness of the barrier layer under equilibrium conditions	See text		
A	Total saturation current as per the Diode Theory	1.096×10^{-8} or 32.88 statamperes	A is the forward direction coefficient calculated in Chapter V	
x_c	Critical thickness below which a barrier can be considered as transparent to charge carriers	See text		

References for Appendix I

1) Radio Engineers Handbook, by F. E. Terman, 1943.

2) Breckenridge and Hosler, Phys. Rev. 41, 793 (1953).

3) Handbook of Chemistry and Physics, 1960.